Detrended Fluctuation Analysis of Spatially Extended Digital Surfaces: the Classification Process of 1/f Noise and Computacional Performance

Vanessa Cristina Oliveira de Souza[a],[b1] and Arcilan Trevenzolli Assireu[b]
[a]National Institute for Space Research, São José dos Campos, SP, Brazil
[b]Federal University of Itajubá, Itajubá, MG, Brazil
Received on Nov 02, 2016 / accepted on Dec 29, 2016

Abstract

A two-dimensional Detrended Fluctuation Analysis (DFA-2D) was employed for the charactarization of $\frac{1}{f}$ classic white, pink and brownian noises. The values were compared with the fBm and fGn fractal signals. The exponent α was evaluated and compared with exponent β of the power spectrum. It was determined that the DFA-2D was capable of detecting and characterizing the different signals. In addition, the relation between α and β was defined as $\beta \equiv 2\alpha - 2$ for two-dimensional signals, with the exception of the fBm signals, where $\beta \equiv 2\alpha$. A computational analysis of the time and accuracy of the DFA-2D was also carried out. The complexity of the method grows exponentially with the enlargement of the image size and the process becomes very slow for images greater than 1000x1000 pixels.

Keywords: long-range dependence, DFA-2D, $\frac{1}{f}$ noise, computational analysis.

1 Introduction

The method employed in the Detrended Fluctuation Analysis (DFA) was formally defined by Peng et al [1] for an analysis of non-stationary signals. In 2002, the method was generalized to characterize multifractal signals[2]. More recently, the DFA and multifractal DFA (MF-DFA) have been expanded to operate not only for a one-dimensional time series but also for any other kind of dimensions, in particular two-dimensional surfaces (DFA-2D and MF-DFA2D)[3]. As well as this, there have been several other suggestions for generalizing the method in recent years [4].

[1]E-mail Corresponding Author: vanessasouza@unifei.edu.br

DFA is regarded as a method that is able to capture the behavior of scales (power law) in long-range correlations in time series, which, in the analysis of signals, is a concept also known as memory or persistence. The DFA' differential is the fact that the method operates in a non-stationary series. If the signal is detrended, it is able to calculate the correlations without being affected by the possible presence of trends. Moreover, as the DFA measures long-range correlations, it is also suitable for calculating what is called the Hurst Exponent [5]. In this way, the fractal theory forms the underlying framework of the DFA.

Although some authors have criticized the method [6, 7, 8, 9], the one-dimensional DFA has been widely used, for example in biomedical [10, 11, 12] and environmental areas [13, 14]. Its multifractal version is also popular, because many of the dynamic processes that occur in nature, cannot be characterized by a single scaling exponent [15, 16, 17].

When applied to two-dimensional surfaces, the notion of persistence can reveal features related to surface roughness. For this reason, DFA-2D and MF-DFA2D have been particularly applied in these conditions. However, although it is an established method for its one-dimensional version, the DFA-2D has not been explored to any extent. Some of its applications can be seen in [18, 19, 20, 21, 22, 23, 24].

One important factor that should be mentioned is that some authors use a one-dimensional DFA to operate within a two-dimensional matrix [25, 26, 27]. The main reasons given by these authors is the high computational cost of the DFA-2D and the difficulty of interpreting the results.

Most of the works in the literature only use the DFA-2D as a computer operator, without being particularly concerned about the physical interpretation of the results. In addition, theoretical studies in general are carried out with knowingly defined fractal data such as the Fractional Brownian Motion (fBm) and the Fractional Gaussian Noise (fGn).

In light of this, this study seeks to assist in the understanding and interpretability of the DFA-2D, by examining the two-dimensional DFA through a canonical data model that includes both fractal and $\frac{1}{f}$ noises ande the relation between the exponent of the DFA-2D (α), with that of the 2D Power Spectrum (β). Another aim of this work was to assess the computacional performance of DFA-2D with different image sizes and different Hurst exponents.

This study is structured in the following way: Section 2 provides a short review of the data used in the research. Section 3 describes the DFA-2D algorithm and the data classification process, as well as conducting a computational analysis. Section 4 concludes the study and adds some final

considerations.

2 $\frac{1}{f}$ Noise Data

[28] states that several physical systems have some type of power-law correlations in space (fractal) or time ($\frac{1}{f^{\gamma}}$). [29] define 1/f noise as a kind of temporal fluctuation which has an intensity and power that are inversely proportional to frequency. The noises of the 1/f type vary their correlation power between the white ($\frac{1}{f^{0}}$) and the brownian noise($\frac{1}{f^{2}}$). There are several other noises between these two extremes, including the intermediary pink noise ($\frac{1}{f}$), which contains influences that are equal to all the intervals of the time scale in the whole spectrum [30].

In contrast with the white noise that does not have memory, the brownian processes are dominated by their recent history. Both are non-stationary. The pink noise shares properties with the white and brownian noises and is considered to be non-stationary and as a result of these intermediary features is the most widely used model to design real events.

When in two-dimensional space, these concepts can be extended to spatial autocorrelation, which is defined as the correlation between pairs of separate points by use of distance. [31] explains that the fractals have a form that is simple but important for the spatial structure, since their patterns are statistically equivalent in all the scales. Thus, the $\frac{1}{f^{\gamma}}$ family of noise models can be regarded as fractional brownian motion, with the exception of $\gamma \equiv 1$ [30]. In this case the range of possible values for γ is altered. Brownian fractional motion are defined by low frequencies, with $1 < \gamma < 3$, including the ordinary brownian motion ($\gamma = 2$). However, the processes derived from fractional gaussian noises are defined by high frequencies, with $-1 < \gamma < 1$, including the white gaussian noise ($\gamma = 0$) [32].

The data regarding white gaussian, pink and brownian noises used in this study, were generated through the Matlab code by [33], based on the methodology described in [31], and using the Inverse Fourier Transform. The size of the matrices was 500x500. Five hundred samples of each model were produced.

Figure 1 shows a sample of each model and its respective power spectrum. Since it is two-dimensional, the exponent β is calculated by means of a radial average and in this case, it expresses the average of the 2D Fourier power spectrum in all possible directions [34]. The Matlab code distributed by [35] was used for power spectrum computation.

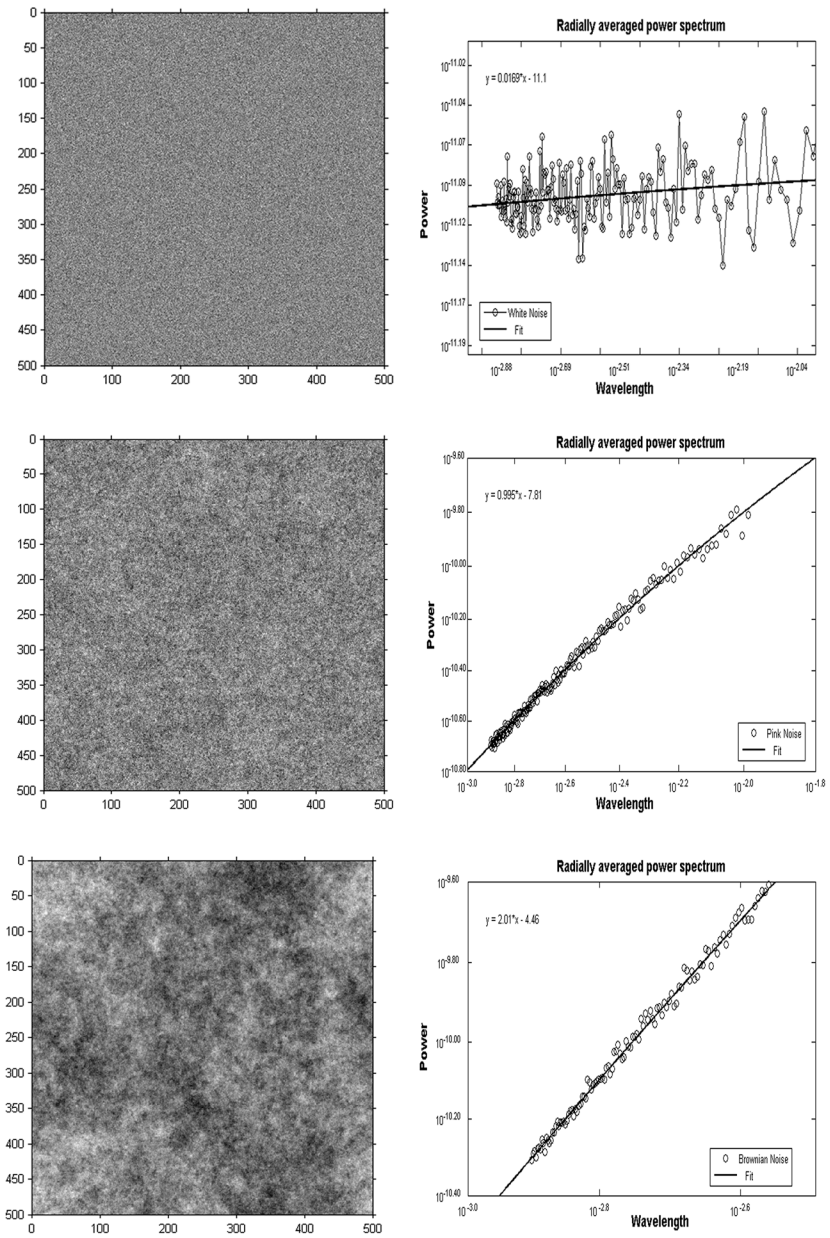

Figure 1: Examples of noisy surfaces and their respective radial power spectrum. At the top, white noise. In the middle, pink noise and down, Brownian noise.

Signal	$\beta_{\mathbf{mean}}$
White Noise	-0.0009 ± 0.0083
Pink Noise	1.0022 ± 0.0080
Brownian Noise	2.0051 ± 0.0074

Table 1: Power spectrum values for the radially averaged power spectral density for some typical signals. The mean and standard deviation are relative to five hundred samples of each model.

Table 1 shows the average values and respective deviations of the power spectrum. It was confirmed that the values obtained are identical to those usually described in the literature for the one-dimensional time series. In the case of simulations of fBm data, when the Hurst exponent = 0.5, $\beta = 2.7597 \pm 0.094$ was obtained. As for fGn signals also with Hurst exponent = 0.5, $\beta = -0.9839 \pm 0.0134$ was obtained.

3 Detrended Fluctuation Analysis 2D (DFA-2D)

3.1 The DFA-2D Algorithm

The implementation of the DFA-2D method is an adaptation of the DFA method for a one-dimensional temporal series and will be described below, as defined in [3].

In the 2D adaptation, the matrix is subdivided into submatrices that range from 6 to (n/4), n being the lowest value between (M/4) e (N/4), where M and N correspond to the number of lines and columns of the matrix respectively. After the subdivision of the matrix, it is integrated in accordance with Equation 1.

$$y_{v,w}(i,j) = \sum_{k_1=1}^{i} \sum_{k_2=1}^{j} X_{v,w}(k_1,k_2) \tag{1}$$

The local trend is removed for each sub-matrix. The least-squares method is employed by adjusting the surface by one of the surface equations defined in [3]. Following this, the residual matrix between the sub-matrix (y) and the adjusted surface ($\tilde{y}$) is calculated (Equation 2).

$$z_{v,w}(i,j) = y_{v,w}(i,j) - \widetilde{y}_{v,w}(i,j) \tag{2}$$

The local fluctuation function for each scale s ($6 \leq s \leq min((M,N)/4)$) is calculated by means of Equation 3.

$$F^2(u,v,s) = \frac{1}{s^2} \sum_{i=1}^{s} \sum_{j=1}^{s} (z_{v,w}(i,j))^2 \tag{3}$$

The global fluctuation function is calculated as an average of the local fluctuation functions, by means of Equation 4.

$$F_2(s) = \left(\frac{1}{p * q} \sum_{i=1}^{p} \sum_{j=1}^{q} F^2(u,v,s) \right)^{\frac{1}{2}} \tag{4}$$

where: p $= M/s$ and $q = N/s$.

Thus by varying the value of s, it is possible to determine the relation of the scale between the fluctuation of the $F_2(s)$ function and the size of Scale s, by means of Equation 5:

$$F(s) \sim s^{\alpha} \tag{5}$$

The exponent for fluctuation scaling (α) is thus calculated as the slope of the straight line of the log-log graph between $F_2(s)$ and s.

3.2 The exponent α

According to some authors, one of the drawbacks of the DFA is the interpretability of exponent α. Since the DFA is used as an approximation for the Hurst exponent, the interpretation in the literature generally follows the pattern of Table 2, which, in reality, describes the possible values and interpretations of the Hurst exponent. The exponent α does not only range between 0 and 1. In general terms [36, 37]:

- If the signal is a fractional gaussian noise (fGn), i.e. is stationary, then $H \equiv \alpha$.
- If the signal is a fractional brownian motion (fBm), i.e. is not stationary, then $H \equiv \alpha - D$, where D is the fractal dimension of the analyzed data.

This relationship arises from the first stage of the DFA algorithm, relative to the integration of the signal. The DFA acts on the fBm signals and the integration turns a possible fGn signal into a fBm and a fBm into an accumulated fBm [37, 38].

α	**Interpretation**
0<a <0.5	Signal with long-range anti-persistence correlation. The closer to zero the higher the anti-persistence.
a = 0.5	Uncorrected signal (white noise)
0.5 <a <1	Signal with persistent long-range correlation. The closer to 1, the greater the persistence.
a = 1	Pink noise
a = 1.5	Brownian noise

Table 2: Values and interpretation of the exponent α

Hence, the stationary signals return values of α between 0 and 1 for the DFA-2D, whereas the non-stationary signals return values between 2 and 3. Values of α between 1 and 2 indicate that the signal does not possess memory. An understanding of the significance of the value of α helps to understand not only the correlation of the signal power analyzed, but also its origins.

In the case of a one-dimensional series, [39] defined the power spectrum β [40] as the equivalent of $\beta = 2H + 1$, for fBm signals and $\beta = 2H - 1$ for fGn signals. [41, 39] provide an experimental validation of the relation between β and α, both for fBm, and for fGn, as:

$$\beta \equiv 2\alpha - 1 \tag{6}$$

3.3 Implementation of the DFA-2D

The code was designed with the aid of Python language and in particular the NumPy and SciPy [42]. Python version 3.4, was used together with numPy 1.11 and sciPy 0.17. NumPy does not have direct functions for calculating the two-dimensional least squares in the matrix. In view of this, a LU factorization was employed to carry out the detrending of each sub-matrix on the basis of the plane model $\widetilde{y}_{v,w}(i,j) = ai + bj + c$.

The DFA-2D was evaluated in scales ranging from 6 to 128. The empirical tests were carried out on a desktop, with a Core i7 processor 950, 3.07 GHZ, 8GB of RAM memory, Linux Centos logrotate 7.2.15.11, with totally dedicated servers.

The experiment conducted by [3] was reproduced as it is, to validate if the method had been implemented correctly i.e. by varying the Hurst exponent between 0.05 0.95, with increments of 0.05. 500 simulations of fBm fractals were produced for each value of the Hurst exponent with dimensions of 500x500, and using Fraclab [43]. The graph in Figure 2 shows the results.

The error bar shows the standard deviation of the 500 samples of each value of H. Thus as stated by [3], the standard deviation increases with the increase of H.

The Python code is available at: https://github.com/vanessavcos/DFA-2D.

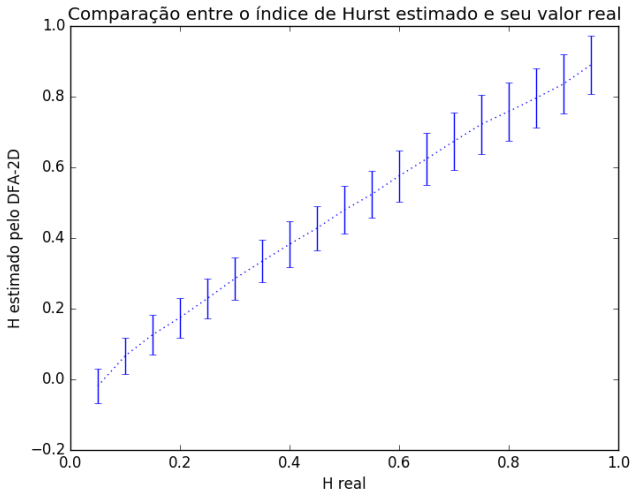

Figure 2: Mean value of the Hurst exponent estimated with the DFA-2D for fBm surfaces.

3.4 Process of Classification

Figure 3 and Table 3 show the log-log graph and the respective values of α for fGn and fBm with the Hurst exponent 0.5 and white ($\beta = 0$), pink ($\beta = 1$) and brown ($\beta = 2$) noises. The values are the averages of the five hundred samples of each model. The fGn data were produced by the successive differences of the respective fBm, in accordance with [36, 37].

From the value of Table 3, it was determined that the DFA-2D was able to discriminate between the different types of signals. It was also found that the α for the white and brownian noises have border values (approximately 1 and 2, respectively) and reveal a close relationship with each other because the brownian noise is the integration of white noise. An important point is the evaluation of the DFA-2D for $(1/f)$ pink noises. The α is given a value of approximately 1.5, which reveals brownian signals for the DFA-1D. It should be noted that the DFA-2D returns values between 1 and 2 for noises

Signal	**Parameter**	α_{mean}
fGn	Hurst = 0.5	0.4067 ± 0.0205
fBm	Hurst = 0.5	2.4794 ± 0.0676
White Noise	$\beta = 0$	0.9992 ± 0.0207
Pink Noise	$\beta = 1$	1.4895 ± 0.0313
Brownian Noise	$\beta = 2$	1.9820 ± 0.0434

Table 3: Mean values of α to some typical signals obtained with DFA-2D. The mean and standard deviation are relative to five hundred samples of each model.

and that, in this case, there is no way to derive the Hurst exponent.

The fBm signal had a value very close to the expected (≈ 2.5). The fGn dispersed a little from the expected (≈ 0.5), which might be a reflection of the methodology employed to derive it from the fBm.

The log-log graph (Figure 1) makes clear the monofractality of the data because the linear regression is a straight line. A structural difference is also found between a fractionary gaussian noise (fGn) and an ordinary gaussian noise (white noise). The fGn shows the same value of the fluctuation function in all the scales because it is a stationary signal.

When the data from Table 1 and Table 3 are compared, it is found that the relation shown in eq. 6 cannot be confirmed. Instead of this, it can be said that for two-dimensional signals $\beta \equiv 2\alpha - 2$ and therefore, $\alpha \equiv \frac{\beta}{2} + 1$ for noises and fGn signals. In the case of fBm signals, it can be approximated that $\beta \equiv \alpha$. However, in the case of the fBm signal when the Hurst exponent = 0.5, the power spectrum overestimates the value of H and hence, the value of α, because the value obtained for β was 2.7, when it should have been equal to 2.5. Tests with other values of the Hurst exponent were carried out and these confirmed the relation of $\beta \equiv \alpha$ for the two-dimensional fBm.

3.5 Computational Performance

This section has evaluated the relation between the processing time, the accuracy of the DFA-2D and the size of the image. It involved assessing thirty samples of the fBm bi-dimensional process, with different sizes (64, 128, 256, 512, 1024 e 2048) and different Hurst exponents (0.3, 0.5 e 0.8). The results are shown in Table 4.

With regard to accuracy, the images of 64x64 and 2048x2048 were those that had most errors. However, even in small-scale conditions, as in the case of the 64x64 image, the DFA-2D came close to the result expected.

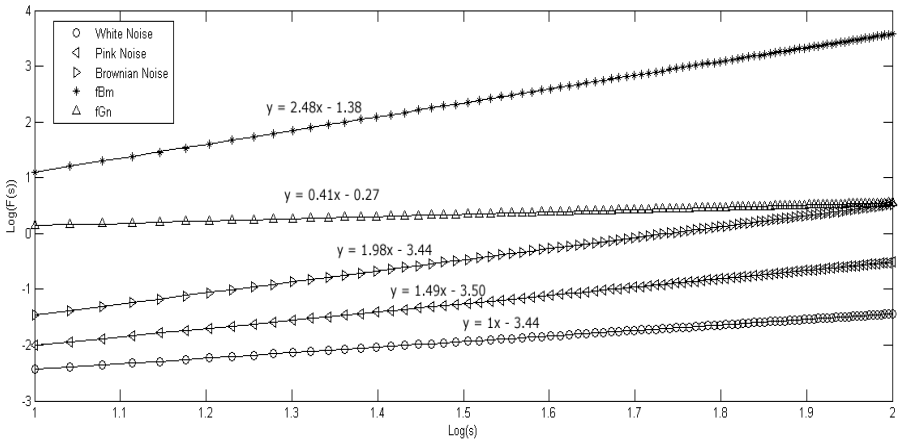

Figure 3: LogLog graphic of typical signals fBm and fGn with Hurst 0.5 and white, pink and Brownian noise. The data are averages of five hundred samples. The highlighted lines and equations refer to the fit of the data. The slope of this line reveals the value of the parameter α.

With regard to performance, it was confirmed in Table 4 and Figure 4 that the enlargement of the image led to an exponential increase in the time. Some authors have drawn attention to the high computational cost of the DFA-2D (asymptotic complexity of the order of $O(n^3)$) [26, 27]. One way to improve performance might be by means of parallelization, since the sub-matrices can be processed in parallel because they do not depend on each other's results. The parallel algorithm that uses GPU and CUDA is under development and will be described shortly. The preliminary results suggest there was a significant improvement in the processing time when the parallel approach was adopted.

4 Concluding Remarks

The DFA is a method that is widely used in several areas. It is important to know the dynamics of data formation, especially in cases of classification. Despite some criticism, several variations of the method have been designed, which is proof of its robustness. However, the DFA-2D version has not been explored to any great extent and there are still very few evaluations with different data from fBm and fGn.

In this study, there is an evaluation of the DFA-2D for white, pink and

		α		Time(s)	
Hurst	**Image Size**	**Mean**	**Std**	**Mean**	**Std**
0.3	64	0.3218	0.0281	0.0911	0.0010
	128	0.3126	0.0129	0.4850	0.0031
	256	0.3030	0.0222	2.3569	0.0048
	512	0.3043	0.0126	11.6196	0.1045
	1024	0.3034	0.0094	59.9468	0.1172
	2048	0.2987	0.0545	357.1790	119.3266
0.5	64	0.5204	0.0403	0.0910	0.0013
	128	0.5037	0.0245	0.4837	0.0010
	256	0.5071	0.0256	2.3583	0.0127
	512	0.4954	0.0186	11.5791	0.0562
	1024	0.5033	0.0123	59.8843	0.0904
	2048	0.4989	0.0913	253.8633	146.4943
0.8	64	0.7892	0.0628	0.0911	0.0021
	128	0.8122	0.0445	0.4849	0.0028
	256	0.8054	0.0262	2.3574	0.0122
	512	0.8020	0.0271	11.5651	0.0176
	1024	0.8043	0.0268	59.8982	0.2121
	2048	0.7880	0.0150	356.1359	148.3523

Table 4: Mean and standard deviation of DFA-2D parameter α and the processing time for images with different sizes and different Hurst exponents.

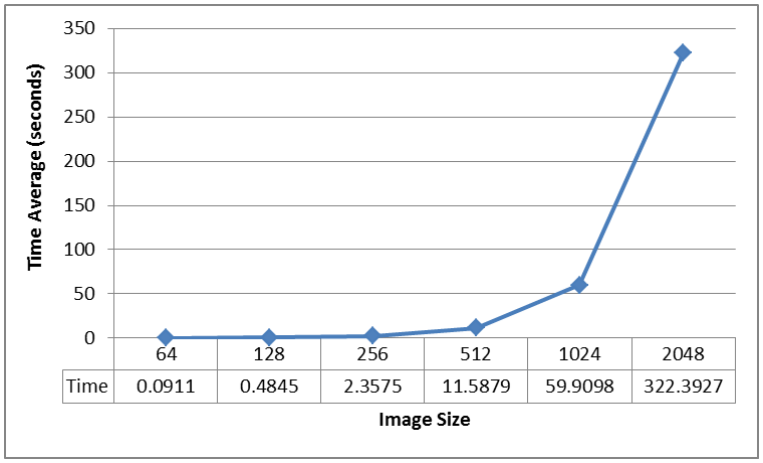

Figure 4: Average processing time values for different image sizes.

brownian noises. It was found that the classical relationship between α and β is not valid for the data analyzed in this study where the exponents cited were related in the form $\beta = 2\alpha - 2$, with the exception of the fBm signal, where $\beta \equiv \alpha$.

The average time for the data processing (512 x 512) is about 12 seconds for the DFA-2D, in a totally dedicated Linux machine. This high complexity of the algorithm has led some sectors to adjust it or even avoid using the method. For this reason, the parallelization of the DFA-2D have been examined and the preliminary results from the use of GPU and CUDA have shown a significant improvement in the results.

In the case of fBm signals, the accuracy of the method is not greatly influenced by the image size. Even with small scales, such as in the image of 64x64, the DFA-2D was able to come close to the result expected.

It was found that the DFA-2D was able to classify and characterize the different systems studied and allow different signals to be identified. Another valuable finding of the work is in the theoretical and practical understanding of the white noise. It could be noted that, despite being decorrelated, the two-dimensional signals with $\beta = 0$ (noise), $\alpha = 0.5$ (fGn) and $\alpha = 2.5$ (fBm), can physically identify different processes.

Acknowledgments. The authors would like to express their gratitude to Professor Reinaldo Rosa (National Institute of Spatial Research Laboratory for Computational and Applied Mathematics (LAC)) for his support in this research undertaking.

References

[1] C. Peng, S. Buldyrev, A. Goldberger, S. Havlin, F. Sciortino, M. Simons, and H. Stanley, "Long-range correlations in nucleotide sequences," *Phys. Rev. E*, vol. 49, pp. 1685–1689, 1994.

[2] J. W. Kantelhardt, S. A. Zschiegner, E. Koscielny-Bunde, S. Havlin, A. Bunde, and H. E. Stanley, "Multifractal detrended fluctuation analysis of nonstationary time series," *Physica A*, vol. 316, no. 1-4, pp. 87–114, 2002.

[3] G.-F. Gu and W.-x. Zhou, "Detrended fluctuation analysis for fractals and multifractals in higher dimensions," *Physical Review*, vol. 74, no. 6, pp. 1–7, 2006.

[4] H. Xiong and P. Shang, "Detrended fluctuation analysis of multivariate time series," *Communications in Nonlinear Science and Numerical Simulation*, vol. 42, pp. 12–21, jan 2017.

[5] H. Hurst, "Long term storage capacity of reservoirs," *Transactions of thr American SOciety of Civil Engineers*, vol. 116, pp. 770–799, 1951.

[6] R. M. Bryce and K. B. Sprague, "Revisiting detrended fluctuation analysis.," *Scientific reports*, vol. 2, p. 315, jan 2012.

[7] Z. Chen, K. Hu, and H. E. Stanley, "Effect of nonstationarities on detrended fluctuation analysis," *Physical Review E*, vol. 65, no. 4, p. 15, 2002.

[8] M. Höll and H. Kantz, "The relationship between the detrendend fluctuation analysis and the autocorrelation function of a signal," *European Physical Journal B*, vol. 88, no. 12, pp. 1–7, 2015.

[9] M. Höll and H. Kantz, "The fluctuation function of the detrended fluctuation analysis - Investigation on the AR (1) process," *European Physical Journal B*, vol. 88, no. 126, pp. 1–15, 2015.

[10] J.-M. Lee, D.-J. Kim, I.-Y. Kim, K.-S. Park, and S. I. Kim, "Detrended fluctuation analysis of EEG in sleep apnea using MIT/BIH polysomnography data," *Computers in Biology and Medicine*, vol. 32, pp. 37–47, jan 2002.

[11] L. Parish, G. Worrell, S. Cranstoun, S. Stead, P. Pennell, and B. Litt, "Long-range temporal correlations in epileptogenic and non-epileptogenic human hippocampus," *Neuroscience*, vol. 125, pp. 1069–1076, jan 2004.

[12] S. L. Winter and J. H. Challis, "Classifying the variability in impact and active peak vertical ground reaction forces during running using DFA and ARFIMA models," *Human Movement Science*, vol. 51, pp. 153–160, jan 2017.

[13] R. G. Kavasseri and R. Nagarajan, "Evidence of crossover phenomena in wind speed data," *Circuits and Systems I: Regular Papers, IEEE Transactions on*, vol. 51, no. 11, pp. 2255–2262, 2004.

[14] K. Koçak, "Examination of persistence properties of wind speed records using detrended fluctuation analysis," *Energy*, vol. 34, pp. 1980–1985, nov 2009.

[15] S. Dutta, D. Ghosh, and S. Chatterjee, "Multifractal detrended fluctuation analysis of human gait diseases," *Frontiers in Physiology*, vol. 4, 2013.

[16] A. Madanchi, M. Absalan, G. Lohmann, M. Anvari, and M. Reza Rahimi Tabar, "Strong short-term non-linearity of solar irradiance fluctuations," *Solar Energy*, vol. 144, pp. 1–9, mar 2017.

[17] E. Maiorino, L. Livi, A. Giuliani, A. Sadeghian, and A. Rizzi, "Multifractal characterization of protein contact networks," *Physica A: Statistical Mechanics and its Applications*, vol. 428, pp. 302–313, jun 2015.

[18] A. V. Alpatov, S. P. Vikhrov, and N. V. Grishankina, "Revealing the surface interface correlations in a-Si:H films by 2D detrended fluctuation analysis," *Semiconductors*, vol. 47, pp. 365–371, mar 2013.

[19] E. Barrera, F. Gonzalez, E. Rodriguez, and J. Alvarez-Ramirez, "Correlation of optical properties with the fractal microstructure of black molybdenum coatings," *Applied Surface Science*, vol. 256, no. 6, pp. 1756–1763, 2010.

[20] Q. Nie, J. Xu, W. Man, and F. Sun, "Detrended fluctuation analysis of spatial patterns on urban impervious surface," *Environmental Earth Sciences*, vol. 74, no. 3, pp. 2531–2538, 2015.

[21] C. Vargas-Olmos, J. S. Murguía, M. T. Ramírez-Torres, M. Mejía Carlos, H. C. Rosu, and H. González-Aguilar, "Two-dimensional DFA scaling analysis applied to encrypted images," *International Journal of Modern Physics C*, vol. 26, no. 08, p. 1550093, 2015.

[22] O. Velazquez-Camilo, E. Bolaños-Reynoso, E. Rodriguez, and J. Alvarez-Ramirez, "Fractal analysis of crystallization slurry images," *Journal of Crystal Growth*, vol. 312, no. 6, pp. 842–850, 2010.

[23] F. Wang, D.-w. Liao, J.-w. Li, and G.-p. Liao, "Two-dimensional multifractal detrended fluctuation analysis for plant identification," *Plant Methods*, vol. 11, no. 12, pp. 1–11, 2015.

[24] R. P. Yadav, S. Dwivedi, A. K. Mittal, M. Kumar, and A. C. Pandey, "Fractal and multifractal analysis of LiF thin film surface," *Applied Surface Science*, vol. 261, pp. 547–553, 2012.

[25] J. Alvarez-ramirez, E. Rodriguez, I. Cervantes, and J. Carlos, "Scaling properties of image textures : A detrending fluctuation analysis approach," *Physica A*, vol. 361, pp. 677–698, 2006.

[26] A. J. EINSTEIN, H.-S. WU, and J. GIL, "Detrended Fluctuation Analysis of chromatin texture for diagnosis in breast cytology," *Fractals*, vol. 10, pp. 19–25, apr 2012.

[27] R. M. de Freitas, P. C. Genovez, M. C. Bentz, R. R. Rosa, and Y. E. Shimabukuro, "Análise de anisotropia de imagens utilizando o método DFA : um estudo de caso na área de exploração de petróleo," in *Anais XIV Simpósio Brasileiro de Sensoriamento Remoto Sensoriamento*, pp. 6463–6470, 2009.

[28] R. F. Voss, "Evolution of long-range fractal correlations and 1/f noise in DNA base sequences," *Physical Review Letters*, vol. 68, no. 25, pp. 3805–3808, 1992.

[29] Gilden, D. Gilden, T. Thornton, and M. Mallon, "1/F Noise in Human Cognition," 1995.

[30] J. M. Halley and W. E. Kunin, "Extinction Risk and the 1/f Family of Noise Models," *Theoretical population biology*, vol. 56, no. 3, pp. 215–30, 1999.

[31] J. J. Lennon, "Red-shifts and red herrings in geographical ecology," *Ecography*, vol. 23, no. 1, pp. 101–113, 2000.

[32] G. Wornell, "Wavelet-based representations for the 1/f family of fractal processes," *Proceedings of the IEEE*, vol. 81, no. 10, pp. 1428–1450, 1993.

[33] J. Yearsley, "spatialPattern," 2016.

[34] R. O. Prum, R. H. Torres, S. Williamson, and J. Dyck, "Coherent light scattering by blue feather barbs," *Nature*, vol. 396, pp. 28–29, nov 1998.

[35] E. Ruzanski, "Radially averaged power spectral density - Matlab code," 2011.

[36] D. Delignieres, S. Ramdani, L. Lemoine, K. Torre, M. Fortes, and G. Ninot, "Fractal analyses for 'short' time series: A re-assessment of classical methods," *Journal of Mathematical Psychology*, vol. 50, no. 6, pp. 525–544, 2006.

[37] A. Eke, P. Hermán, J. B. Bassingthwaighte, G. M. Raymond, D. B. Percival, M. Cannon, I. Balla, and C. Ikrényi, "Physiological time series: Distinguishing fractal noises from motions," *Pflugers Archiv European Journal of Physiology*, vol. 439, no. 4, pp. 403–415, 2000.

[38] B. B. Mandelbrot and J. W. Van Ness, "Fractional Brownian Motions, Fractional Noises and Applications," *SIAM Review*, vol. 10, pp. 422–437, oct 1968.

[39] C. Heneghan and G. McDarby, "Establishing the relation between detrended fluctuation analysis and power spectral density analysis for stochastic processes," *Physical Review E*, vol. 62, no. 5, pp. 6103–6110, 2000.

[40] G. Heinzel, A. Rüdiger, and R. Schilling, "Spectrum and spectral density estimation by the Discrete Fourier transform (DFT), including a comprehensive list of window functions and some new at-top windows.," *Max Plank Institute*, pp. 1–84, 2002.

[41] S. V. Buldyrev, A. L. Goldberger, S. Havlin, R. N. Mantegna, M. E. Matsa, C.-K. Peng, M. Simons, and H. E. Stanley, "Long-range correlation properties of coding and noncoding DNA sequences: GenBank analysis," *Physical Review E*, vol. 51, pp. 5084–5091, may 1995.

[42] Scipy.org, "Numpy and SciPy Documentation," 2016.

[43] INRIA, "FRACLAB, A Fractal Analysis Toolbox for Signal and Image Processing," 2016.